Turbulent $E \times B$ advection of charged test particles with large gyroradii

T. Hauff and F. Jenko

Max-Planck-Institut für Plasmaphysik, EURATOM Association, 85748 Garching, Germany

Abstract.

The turbulent $E \times B$ advection of charged test particles with large gyroradii is investigated. To this aim, a recently developed theory – the so-called decorrelation trajectory method – is used together with direct numerical simulations and analytical calculations. It is found that for Kubo numbers larger than about unity, the particle diffusivity is almost independent of the gyroradius as long as the latter does not exceed the correlation length of the electrostatic potential. The underlying physical mechanisms leading to this surprising and initially counterintuitive behavior are identified.

1. Introduction

The quest to understand the turbulent transport of particles, momentum, and energy in magnetized plasmas may be considered as one of the key challenges in present-day plasma physics. While a lot of progress could be achieved in this area of research over the last few decades, many basic issues are still relatively poorly understood. One such issue is the turbulent $E \times B$ advection of charged test particles with large gyroradii which has important applications both in plasma astrophysics as well as in fusion research. In the latter case, e.g., one is interested in the interaction of α particles or impurities with the background turbulence. To be able to address such topics, a thorough understanding of the dependence of the particle diffusivity on the gyroradius is required. It is the main goal of the present paper to shed new light on this old question, thereby revealing novel insights and allowing for more accurate descriptions of such physical systems.

Provided that the temporal changes of the background potential are slow compared to the gyration period and that the potential amplitudes are not too large, the particles' dynamics may be treated in the spirit of gyrokinetic theory.[1] This means that a gyrating particle is simply replaced by a charged ring. This 'quasiparticle' drifts with an $E \times B$ velocity which is computed from a gyroorbit-averaged potential. Since this process of gyroaveraging always reduces the effective drift velocity, one would naively expect that the resulting particle diffusivity is also reduced. It is one of the key findings of the present work, however, that this conclusion is not justified. In fact, we will be able to show that in a strong turbulence situation, the diffusivity is more or less independent of the gyroradius as long as the latter does not exceed the correlation length of the electrostatic potential. Moreover, the underlying physical mechanisms leading to this initially counterintuitive behavior will be identified.

The present work was inspired, in part, by two recent papers by M. Vlad and co-workers [2, 3] in which they extended the so-called decorrelation trajectory (DCT) method [4, 5] for computing diffusivities from the autocorrelation function of the potential to the case of particles with finite gyroradii. And the results they got were very surprising. In particular, they observed that for sufficiently large Kubo numbers (i.e., for relatively strong turbulence), the diffusivity may *increase* with increasing gyroradius by up to several orders of magnitude. Obviously, this finding is in stark contrast to the usual physical picture sketched above. Therefore, it motivated us to revisit the problem of turbulent $E \times B$ advection of charged test particles with large gyroradii, using both the DCT method and other approaches.

In this paper, we will restrict our studies to a rather simple situation, namely the two-dimensional dynamics of test particles in a homogeneous, static magnetic field and a prescribed electrostatic potential which is stochastic in space and time. Such models have been used in many previous investigations (see, e.g., Ref. [7] and references therein) mainly due to their accessibility in terms of numerical and analytical methods. Although the relation between the diffusivity obtained from the dispersion of test particles and the diffusion coefficient inferred from the self-consistent turbulent flux is not easy to establish [8, 9], the study of test particle dynamics is still considered quite useful, especially if one is dealing with trace species at low density. It is our main goal in the present paper to study the fundamental physical processes in a fairly clean environment. Specific applications to various situations in fusion research or plasma astrophysics, possibly including additional effects, are left for future work.

The dependence of the diffusivity of test particles on the gyroradius ρ has also been the subject of several previous studies beyond the ones already mentioned. E.g., in Refs. [10, 11, 12], finite Larmor radius (FLR) effects were studied for test particles in Hasegawa-Mima turbulence using the gyrokinetic approximation. Here, it was found that "FLR effects strongly inhibit stochastic diffusion" [10], and that the diffusivities drop roughly as ρ^{-1} and $\rho^{-0.5}$ (or $\rho^{-0.35}$) in the low and high Kubo number regimes, respectively.[11] These results are in agreement with naive expectations and shall also be confirmed in the present, more systematic study. Moreover, in a fairly recent investigation of the same basic type, an additional observation was made. Here, the authors find that "as long as ρ is smaller than or similar to the typical size of the [turbulent] structures, FLR effects are irrelevant."[12] In other words, a significant FLR reduction of the diffusivity requires the gyroradius to exceed the correlation length of the potential. While very interesting, this result was not discussed any further, however. In particular, no explanation was given in terms of the underlying physical mechanisms which lead to this behavior, and no mention was made about a possible Kubo number dependence on this effect. In fact, Refs. [11] and [12] seem to contradict each other with respect to the existence of a reduction threshold in ρ. In contrast, the present study offers a much more detailed and systematic investigation of these issues, including the identification of the physical mechanisms at work.

The remainder of this paper is organized as follows. In Section 2, a brief review of the DCT method and its extension to particles with finite gyroradii (as found in the literature) is given. In Section 3, we put forward a modified version of this DCT approach which leads to (even qualitatively) different mechanisms and results. In Section 4, the DCT method itself is compared – for the first time – with direct numerical simulations based on prescribed random potentials. We find that for large Kubo numbers, the effect of particle trapping is generally overestimated by the DCT method, leading to significant discrepancies. In Section 5, a large number

of direct numerical simulations are presented and their dependence on Kubo number and gyroradius is studied. In the limit of small/large Kubo numbers and small/large gyroradii, analytical expressions for the ratio D_ρ/D_0 are derived which agree very favorably with the simulation results. We close with some conclusions in Section 6.

2. A brief review of the decorrelation trajectory (DCT) method

In a series of papers over the last few years, M. Vlad and colleagues developed a novel theory describing the diffusion of charged particles in prescribed electromagnetic fields which has been named decorrelation trajectory (DCT) method.[4, 5] Recently, the DCT approach has been applied to the $E\times B$ drift motion of ions with large gyroradii, yielding very surprising and counterintuitive results.[2, 3] The goal of this section is to briefly review the DCT theory, in particular in relation to the latter problem, thus providing a starting point for a modified DCT approach which will be presented and discussed in the next section. For details, the reader is referred to the original papers.

2.1. The DCT method for $E\times B$ drift motion

In the following, we shall assume the existence of a strong, homogeneous, static magnetic field which points in the z direction, and consider the motion of a charged test particle in a given perpendicular plane. Neglecting finite gyroradius effects, a fluctuating electrostatic potential $\phi(\mathbf{x},t)$ then leads to an $E\times B$ drift velocity which can be written as

$$v_i^{\mathrm{dr}}(\mathbf{x},t) = -\varepsilon_{ij}\frac{\partial\phi(\mathbf{x},t)}{\partial x_j} \tag{1}$$

in dimensionless units. Here, we have used Einstein's summation convention and the notation $(x_1,x_2)=(x,y)=\mathbf{x}$. Moreover, ε_{ij} denotes an antisymmetric tensor of rank two with $\varepsilon_{12}=-\varepsilon_{21}=1$ and $\varepsilon_{11}=\varepsilon_{22}=0$. Particles subject to this kind of dynamics will generally exhibit diffusive motion in the x-y plane. According to the formula by Taylor [13], the corresponding diffusion coefficient in one dimension can be expressed as

$$D_x(t) \equiv \frac{1}{2}\frac{d}{dt}\langle x(t)^2\rangle = \int_0^t d\tau\, L_{xx}(\tau) \tag{2}$$

where

$$L_{xx}(t) \equiv \langle v_x^{\mathrm{dr}}(\mathbf{x}(0),0)\, v_x^{\mathrm{dr}}(\mathbf{x}(t),t)\rangle \tag{3}$$

and the angular brackets denote ensemble averaging over realizations of the (prescribed) electrostatic potential. In other words, the time dependent diffusion coefficient $D_x(t)$ is the time integral over the Lagrangian correlation function $L_{xx}(t)$ of the particle's drift velocity.

The DCT method developed by M. Vlad and co-workers [4, 5, 2, 3] offers a possibility to calculate the Lagrangian correlation function from the corresponding Eulerian correlation function. Here, in contrast to previous attempts to connect these two types of correlations, particle trapping effects are retained. Assuming that the Eulerian autocorrelation function of the potential is given by

$$E(\mathbf{x},t) \equiv \langle \phi(0,0)\,\phi(\mathbf{x},t)\rangle\,, \tag{4}$$

one obtains

$$E_{\phi j}(\mathbf{x},t) \equiv \langle \phi(0,0)\, v_j^{\rm dr}(\mathbf{x},t)\rangle = -\varepsilon_{jn}\frac{\partial E(\mathbf{x},t)}{\partial x_n} \tag{5}$$

and

$$E_{ij}(\mathbf{x},t) \equiv \langle v_i^{\rm dr}(0,0)\, v_j^{\rm dr}(\mathbf{x},t)\rangle = -\varepsilon_{in}\varepsilon_{jm}\frac{\partial^2 E(\mathbf{x},t)}{\partial x_n \partial x_m}\,. \tag{6}$$

The Eulerian correlation function $E_{ij}(\mathbf{x},t)$ defined by Eq. (6) can be used to determine a key quantity characterizing the potential fluctuations, namely the so-called Kubo number [14]

$$K \equiv \frac{V\tau_c}{\lambda_c} = \frac{\tau_c}{\tau_{\rm fl}}\,. \tag{7}$$

Here, τ_c and λ_c denote, respectively, the autocorrelation time and length of the electrostatic potential, V is the mean drift velocity which can be calculated as

$$V = \left(-\frac{\partial^2 E(0,0)}{\partial x^2}\right)^{1/2}\,, \tag{8}$$

and $\tau_{\rm fl}$ is the mean time of flight for a distance of one correlation length. The limits $K\to\infty$ and $K\to 0$ correspond to static and fast fluctuations, respectively. Sometimes, the regime of $K \lesssim 1$ is labeled 'weak turbulence' or 'quasilinear,' while the $K \gtrsim 1$ regime is denoted as 'strong turbulence' or 'nonlinear.' The Kubo number will play an important role in the remainder of this paper.

The fundamental idea of the DCT method is to subdivide the total collection of realizations of ϕ into sets of subensembles $S(\phi^0,\mathbf{v}^0)$ for each of which the initial conditions $\phi(\mathbf{x}(0),0) = \phi^0$ and $v_i^{\rm dr}(\mathbf{x}(0),0) = v_i^0$ are satisfied. Assuming that the corresponding probability distribution function $P_1(\phi^0,\mathbf{v}^0)$ is known, the Lagrangian correlation of the velocity components can be written as

$$\begin{aligned} L_{ij}(t) &\equiv \langle v_i^{\rm dr}(\mathbf{x}(0),0)\, v_j^{\rm dr}(\mathbf{x}(t),t)\rangle = \\ &= \iint d\phi^0\, d\mathbf{v}^0\, P_1(\phi^0,\mathbf{v}^0)\, \langle v_i^{\rm dr}(\mathbf{x}(0),0)\, v_j^{\rm dr}(\mathbf{x}(t),t)\rangle_S = \\ &= \iint d\phi^0\, d\mathbf{v}^0\, P_1(\phi^0,\mathbf{v}^0)\, v_i^0 \langle\, v_j^{\rm dr}(\mathbf{x}(t),t)\rangle_S = \\ &= \iint d\phi^0\, d\mathbf{v}^0\, P_1(\phi^0,\mathbf{v}^0)\, v_i^0\, V_j^L(t;S) \end{aligned} \tag{9}$$

where

$$V_j^L(t;S) \equiv \langle\, v_j^{\rm dr}(\mathbf{x}(t),t)\rangle_S \tag{10}$$

is the mean *Lagrangian* drift velocity in the subensemble S at time t.

On the other hand, the average *Eulerian* drift velocity in the subensemble S is given by [7]

$$\begin{aligned} V_j^E(\mathbf{x},t;S) &\equiv \langle v_j^{\rm dr}(\mathbf{x},t)\rangle_S \\ &= \phi^0\,\frac{E_{\phi j}(\mathbf{x},t)}{E(0,0)} + v_1^0\,\frac{E_{1j}(\mathbf{x},t)}{E_{11}(0,0)} + v_2^0\,\frac{E_{2j}(\mathbf{x},t)}{E_{22}(0,0)}\,, \end{aligned} \tag{11}$$

provided that $P_1(\phi^0,\mathbf{v}^0)$ is a Gaussian distribution. For the average potential in the subensemble S, a similar expression can be found:

$$\begin{aligned} \Phi(\mathbf{x},t;S) &\equiv \langle \phi(\mathbf{x},t)\rangle_S \\ &= \phi^0\,\frac{E(\mathbf{x},t)}{E(0,0)} + v_1^0\,\frac{E_{1\phi}(\mathbf{x},t)}{E_{11}(0,0)} + v_2^0\,\frac{E_{2\phi}(\mathbf{x},t)}{E_{22}(0,0)}\,. \end{aligned} \tag{12}$$

Therefore the mean potential and the mean drift velocity in a given subensemble are connected via

$$V_i^E(\mathbf{x},t;S) = -\varepsilon_{ij}\frac{\partial\Phi(\mathbf{x},t;S)}{\partial x_j} \tag{13}$$

which is the subensemble analogue of Eq. (1).

At this point, the key concept of a 'decorrelation trajectory' is introduced. By the latter, one means the solution $\mathbf{X}(t;S)$ of the equation

$$\frac{dX_i}{dt} = V_i^E(\mathbf{X},t;S) = -\varepsilon_{ij}\frac{\partial\Phi(\mathbf{X},t;S)}{\partial X_j} \tag{14}$$

for appropriate initial conditions. Decorrelation trajectories are then used in order to express $V_j^L(t;S)$ in terms of $V_j^E(\mathbf{x},t;S)$ via the Ansatz

$$V_j^L(t;S) \cong V_j^E(\mathbf{X}(t;S),t;S)\,. \tag{15}$$

Using this assumption, Eqs. (2) and (9) can be rewritten as

$$D_x(t) = \iint d\phi^0\, d\mathbf{v}^0\, P_1(\phi^0,\mathbf{v}^0)\, v_x^0\, X(t;S)\,. \tag{16}$$

In practice, Eq. (16) is evaluated numerically, approximating the integral by a sum over a discrete number of subensembles. Since the subensemble-averaged potential Φ tends to be much smoother than a real potential ϕ, and it typically decays to zero for large distances or times (i.e., when the correlation functions vanish), it is often sufficient to retain a fairly limited number of decorrelation trajectories. This may be considered the main advantage of the DCT method. However, its drawback is that Eq. (15) cannot be derived from first principles. In Ref. [4], the authors state that it is justified indirectly since the DCT approach is able to reproduce some characteristic features like the 'percolation scaling' for high Kubo numbers.[17] And in Ref. [6], the usual DCT method is refined by introducing subensembles which differ in higher order derivatives of the electrostatic potential. Only small corrections for the diffusion coefficient are found, leading to the claim that the results of the DCT method are thus – in some sense – validated. Nevertheless, a test of the DCT method via comparisons with direct numerical simulations has not yet been done. This gap will be closed in Section 4.

2.2. The extension of the DCT method to particles with finite gyroradii

As is obvious from the above derivation, the DCT method makes use of the fact that the particle's velocity is given by the $E\times B$ drift. However, in Ref. [2] the authors postulate the possibility of an extension of the DCT approach to particles with finite gyroradii by solving the exact Lorentz equation using the subensemble-averaged potential. They define the average position of the gyrocenter in the subensemble, $\mathbf{\Xi}(t;S) \equiv \langle\xi(t)\rangle_S$, and the average gyroradius in the subensemble, $\mathbf{\Pi}(t;S) \equiv \langle\rho(t)\rangle_S$. Then they define new decorrelation trajectories by solving the Lorentz differential equation

$$\begin{aligned}\frac{d\Xi_i}{dt} &= -\varepsilon_{ij}\frac{\partial\Phi(\mathbf{\Xi}+\mathbf{\Pi},t;S)}{\partial\Xi_j}\,,\\ \frac{d\Pi_i}{dt} &= \varepsilon_{ij}\left[\frac{\partial\Phi(\mathbf{\Xi}+\mathbf{\Pi},t;S)}{\partial\Xi_j}+\Pi_j\right]\,.\end{aligned} \tag{17}$$

Here, the initial conditions

$$\Pi_1(0) = \rho\cos\varphi\,, \quad \Pi_2(0) = \rho\sin\varphi\,, \quad \Xi_i(0) = -\Pi_i(0) \tag{18}$$

are used. They imply that the particles start at the origin. The diffusion coefficient is calculated by replacing $X(t;S)$ by $\Xi_x(t;S)$ in Eq. (16) and additionally varying the angle φ.

Solving these equations, a *strong increase* of the diffusion coefficient with increasing gyroradius has been found for high Kubo numbers.[2, 3] This result is very surprising and counterintuitive. Particles with finite gyroradii 'see' a gyroaveraged – and therefore reduced – effective potential, and this should lead to a reduced effective $E\times B$ drift, associated with *lower* diffusivities. This apparent contradiction has been a key motivation for the present work. We will approach the present problem in two consecutive steps. First, we will reconsider the DCT-based approach that was just described (Section 3). Then, we will perform and examine direct numerical simulations of particles with finite gyroradii in prescribed time-dependent electrostatic potentials (Section 4 and 5). At the end of this dual task, a coherent picture will have emerged which corrects *both* the naive expectations *and* the previous DCT-based results.

3. A modified DCT approach for particles with finite gyroradii

Let us start the discussion and modification of the above DCT approach for particles with finite gyroradii by pointing out again that Eq. (17) is simply an *ad hoc* Ansatz which has not been derived from first principles. Moreover, the use of the subensemble-averaged potential Φ in the Lorentz differential equation seems hard to justify since it is based on the assumption of vanishing gyroradii. These facts indicate that it is worth reinvestigating the DCT approach outlined above. In the following, we will show that it actually should be corrected, and how.

3.1. Two ways of gyroaveraging

As is shown in Ref. [3], the Lorentz approach based on Eq. (17) can be replaced by an alternative, 'gyrokinetic' approach. Here, the subensemble potential is averaged over the gyroorbit of the particle, so that

$$\Psi(\boldsymbol{\Xi},\rho,t;S) \equiv \frac{1}{2\pi}\int_0^{2\pi} d\varphi\,\Phi(\boldsymbol{\Xi}+\rho(\varphi),t;S) \tag{19}$$

is employed in lieu of Φ. Using Eq. (12), it then follows that this amounts to replacing the Eulerian correlation function $E(\mathbf{x},t)$ by its gyroaverage,

$$E^{\mathrm{eff,A}}(\mathbf{x},\rho,t) \equiv \frac{1}{2\pi}\int_0^{2\pi} d\varphi\,E(\mathbf{x}+\rho(\varphi),t)\,. \tag{20}$$

The DCT method can then be applied to this new effective autocorrelation function as shown in the last section. The denominators in Eq. (12) are not affected since they are constants. In Ref. [3], it has been demonstrated that there is good agreement between the original DCT method based on the Lorentz differential equation and the present gyrokinetic approximation. For later use, we also provide the following representation of $E^{\mathrm{eff,A}}$ as a Fourier integral:

$$E^{\mathrm{eff,A}}(\mathbf{x},\rho) = \frac{1}{(2\pi)^2}\int_{-\infty}^{\infty} d\mathbf{k}\,e^{i\mathbf{k}\cdot\mathbf{x}}E(\mathbf{k})\,J_0(k\rho)\,. \tag{21}$$

Here, the time dependence has been suppressed, $E(\mathbf{k}) \equiv \mathcal{F}\{E(\mathbf{x})\}$ denotes the Fourier transform of $E(\mathbf{x})$, and J_0 is the Bessel function of order zero. In the following, we will derive a different type of effective autocorrelation function, however, which is in line with the physical principles underlying the $E\times B$ advection of particles with finite gyroradii.

The standard gyrokinetic approach consists in first gyroaveraging the potential and then computing the corresponding $E\times B$ drift velocity from this new effective potential. This means, it is possible to bring the finite gyroradius problem into the form of the zero gyroradius one if the original potential is replaced by

$$\langle\phi\rangle(\mathbf{x}) \equiv \frac{1}{(2\pi)^2}\int_{-\infty}^{\infty} d\mathbf{k}\, e^{i\mathbf{k}\cdot\mathbf{x}}\, \phi(\mathbf{k})\, J_0(k\rho) \tag{22}$$

where $\phi(\mathbf{k}) \equiv \mathcal{F}\{\phi(\mathbf{x})\}$. The corresponding Eulerian autocorrelation function $E^{\mathrm{eff,B}}$ then reads

$$E^{\mathrm{eff,B}}(\mathbf{x},\rho) = \frac{1}{(2\pi)^2}\int_{-\infty}^{\infty} d\mathbf{k}\, e^{i\mathbf{k}\cdot\mathbf{x}}\, E(\mathbf{k})\, J_0^2(k\rho) \tag{23}$$

where we have used the well-known convolution theorem. We note that we employ an index 'B' for this new effective autocorrelation function and an index 'A' for the effective autocorrelation function expressed by Eq. (21). These two methods differ in that the Bessel functions enter, respectively, squared and linearly. In this context, it is crucial to point out once again that method B is in line with the standard gyrokinetic approach while method A is not.

Given the above effective Eulerian correlations, the DCT method can then be applied as usual. One only has to take into account that the denominators of Eq. (12) must be replaced by the corresponding effective values. Moreover, using method B, the starting points for the gyrocenters are at the origin. According to method A, however, they lie on a circle of radius ρ around the origin since the particles themselves start at the origin.

3.2. Comparison of the two methods

Next, we compare these two methods of calculating the diffusion coefficient for finite gyroradii by assuming a simple autocorrelation function of the form

$$E(\mathbf{x},t) = A\, e^{-x^2} e^{-(t/\tau_c)^2}\,. \tag{24}$$

Here, distances are expressed in units of the correlation length λ_c, and τ_c denotes the correlation time (time is still expressed in units of gyration periods). The Kubo number K can be controlled by varying τ_c. Choosing the form of Eq. (24) for $E(\mathbf{x},t)$ has two main advantages. First, due to spatial isotropy, one can save one dimension in the integral over the subensembles in Eq. (16). Second, due to the factorization of space and time correlations, it is possible to relate the two quantities $D(t, K\to\infty)$ and $D(t\to\infty, K)$ to each other as is shown in Ref. [5]. In other words, the long-time limit of the diffusivity for different Kubo numbers can be computed from the time-dependent diffusivity in a static potential. It is thus possible to obtain continuous curves of the quantity $D(K) \equiv D(t\to\infty, K)$. Some examples are shown in Fig. 1. Here, the underlying equations of motion have been solved numerically via a fourth-order Runge-Kutta method. The number of subensembles has been chosen such that the curves are sufficiently smooth. Only in the high Kubo number regime, small oscillations can be observed in some of the curves, reflecting the limited number of

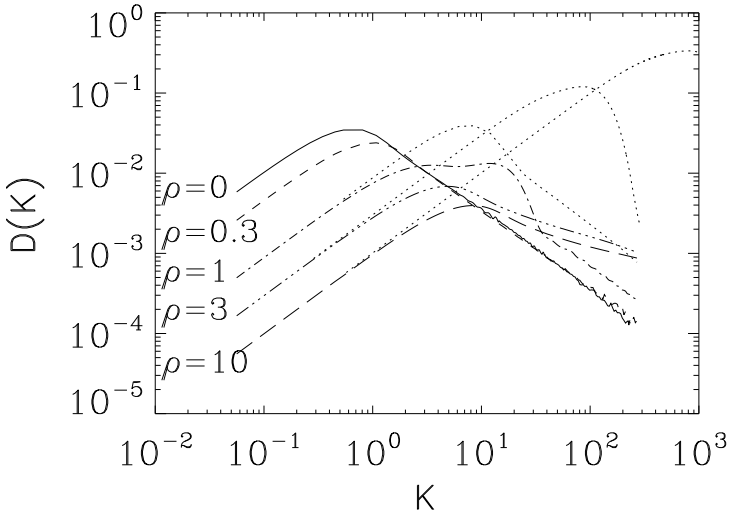

Figure 1. Diffusion coefficient D for $t \to \infty$ as a function of the Kubo number K for different gyroradii ρ (normalized to the correlation length of the potential). The solid/dashed and dotted lines represent numerical calculations with the DCT method using, respectively, $E^{\mathrm{eff,B}}$ and $E^{\mathrm{eff,A}}$.

subensembles. The $D(K)$ curves have been computed for gyroradii of 0, 0.3, 1, 3 and 10 times the correlation length of the potential. Dashed lines represent the diffusion coefficient calculated with the effective correlation $E^{\mathrm{eff,B}}$, whereas dotted lines denote the diffusion coefficient using $E^{\mathrm{eff,A}}$. The results for method A are practically identical to those published in Ref. [3] although the time dependence of the correlation function is somewhat different. In particular, one observes huge enhancements of the maximum diffusivity with increasing gyroradii. This surprising and very counterintuitive finding is modified in a significant fashion when method B is employed instead. While for low Kubo numbers, both methods agree, the increase of the diffusion coefficient with increasing gyroradii in the high K regime is still existent but much more moderate. Moreover, while this increase of the diffusion coefficient is due to the extension of the 'linear regime' to larger K for method A, it is rather due to a more moderate decay of $D(K)$ with increasing K for method B. In the next subsection, we will give an explanation for these findings.

3.3. $D(K)$ curves and effective correlation functions

The spatial part of the effective autocorrelation function $E^{\mathrm{eff,A}}$ for different gyroradii ρ (normalized to the correlation length of the potential) is shown in Fig. 2. Due to spatial isotropy, one obtains the respective two-dimensional surfaces by rotating these curves around the symmetry axis. The maxima of the effective correlation functions lie on a ring with radius ρ. This is because to obtain $E^{\mathrm{eff,A}}$, the original correlation function for $\rho = 0$, which has its maximum in the center, is gyroaveraged. Thus for $x = \rho$, the 'ring' over which the gyroaverage is calculated goes straight through the maximum of the latter. As mentioned in Section 2, the decorrelation trajectories start

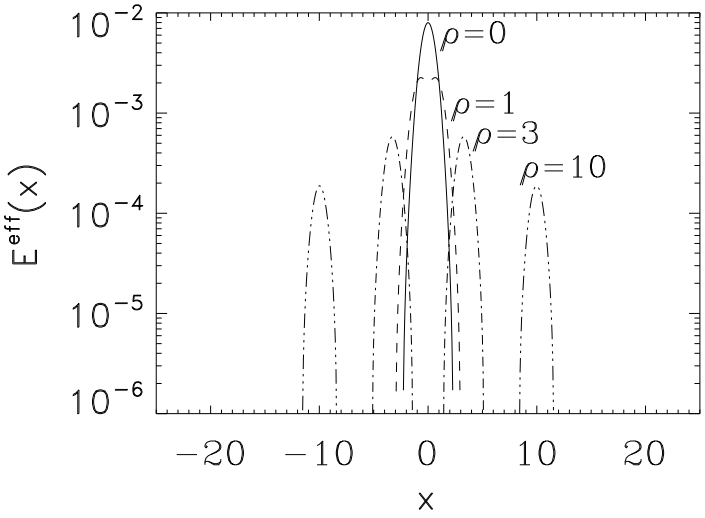

Figure 2. Spatial part of the effective autocorrelation function $E^{\mathrm{eff,A}}$ for different gyroradii ρ (normalized to the correlation length of the potential).

at a distance ρ from the origin, i.e., at the maximum of the correlaton function. Since the average subensemble potential is constructed as a superposition of $E^{\mathrm{eff,A}}$ and its derivatives [see Eq. (12)], it can be shown that shape of the equipotential lines and therefore the shape of the decorrelation trajectories is similar to the ring structure of $E^{\mathrm{eff,A}}$. Therefore the drastic increase of the diffusivity results from the fact that the effective correlation function supports much wider trajectories than the original one. On the other hand, the absolute values of $E^{\mathrm{eff,A}}$ are reduced, leading to a reduced particle velocity and therefore to the extension of the linear regime to higher values of K. A similar explanation was given in Ref. [3]. There it was also shown that the effective time of flight over a distance of one correlation length scales like $\tau_{\mathrm{fl}}^{\mathrm{eff}} \propto \rho^2$. Since the diffusion coefficient takes on its maximum value at $\tau_{\mathrm{fl}} = \tau_c$, it follows that the position of the maximum of $D(K)$ moves towards larger K like ρ^2.

Now we turn to the effective autocorrelation function $E^{\mathrm{eff,B}}$ which is plotted in Fig. 3. We note that its shape differs completely from that of $E^{\mathrm{eff,A}}$. While the main maximum remains at the origin, additional side maxima occur at $|x| = 2\rho$. This behavior becomes clear if we recall that gyroaveraged potentials are used to calculate the autocorrelation function. Since the gyroaveraging is done over rings with radius ρ around certain points, it is obvious that the autocorrelation is maximal if the two rings are tangent to each other, i.e., for $|x| = 2\rho$. In this case, the correlated area increases along with the autocorrelation. [According to method B, the decorrelation trajectories start at the origin.]

Although the maximum value of $E^{\mathrm{eff,B}}$ decreases with increasing gyroradius, the diffusivity is again observed to increase – at least moderately (see Fig. 1). However, the underlying physical mechanism is completely different from the one identified for method A. In case B, it is the widening of the effective autocorrelation function which is responsible for the increase of the diffusive transport. Although the average drift velocity is reduced, the autocorrelation $E^{\mathrm{eff,B}}$ as well as its derivatives remain nonzero

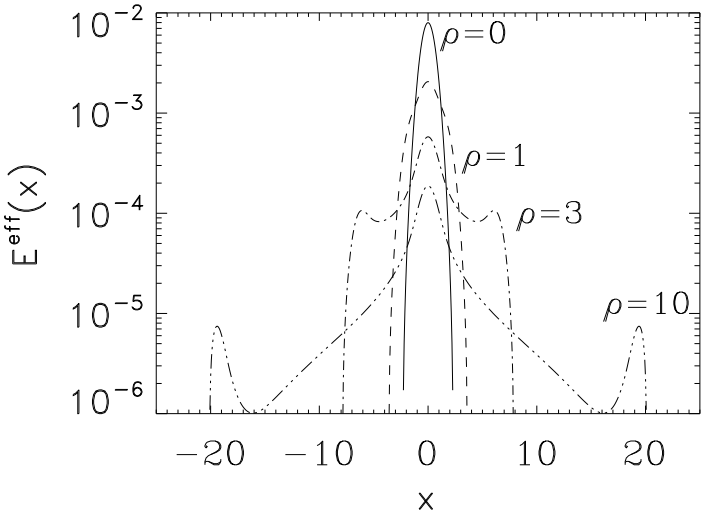

Figure 3. Spatial part of the effective autocorrelation function $E^{\mathrm{eff,B}}$ for different gyroradii ρ (normalized to the correlation length of the potential).

over a larger area in space, leading to larger excursions of the equipotential lines and therefore to more extended decorrelation trajectories. This is in line with the finding that a more moderate decay of the autocorrelation in space leads to a slower reduction of the diffusion coefficient for large and growing Kubo numbers.[5] Due to this widening effect, the curves for different gyroradii in Fig. 1 are actually able to intersect.

As can be inferred from Fig. 3, the correlation length – defined here as the e-folding length of E^{eff} – stays approximately the same for $\rho \gtrsim 1$. Moreover, the envelope of the Bessel function $J_0(k\rho)$ is given by $(\pi k\rho/2)^{-1/2}$ for $k\rho \gg 1$, and therefore the mean drift velocity $V^{\mathrm{eff}} = \sqrt{E_{ii}^{\mathrm{eff}}(0,0)}$ scales like $\rho^{-1/2}$. Consequently, the effective time of flight scales like $\tau_{\mathrm{fl}}^{\mathrm{eff}} \propto \rho^{1/2}\tau_{\mathrm{fl}}$, and the maxima of the curves $D(K)$ move to the right like $\rho^{1/2}$. This prediction is confirmed by Fig. 1. The $\rho^{1/2}$ dependence of the position of the maxima is much weaker than the ρ^2 dependence obtained for method A. This is why the extension of the linear regime is weaker and therefore the maxima of $D(K)$ are reduced compared to method A. The fact that one still finds an increase of transport in the high Kubo number regime for method B has to do with the reduced decrease of $D(K)$ rather than with the displacement of the maximum.

Finally, it is also possible to explain why both methods lead to the same results for $K \lesssim 1$. In this regime, the decorrelation of the particles is temporal. Therefore, in the language of the DCT method, the particles are not able to explore large regions of the subensemble potential before being decorrelated. Consequently, the dynamics of the particles is dominated by the behavior of E^{eff} around the origin. And it can be shown that $E^{\mathrm{eff,A}}(|\rho|) = E^{\mathrm{eff,B}}(0)$. This means that the differences between method A and B only appear if the particles can travel sufficiently far away from the origin, i.e., for high Kubo numbers.

In summary, we have shown in this section that the diffusion of particles with finite gyroradii needs to be treated in the framework of a DCT approach which is

based on autocorrelation functions of gyroaveraged potentials. Such a theory leads to a significant reduction of the maximum diffusivities compared to the results presented in Refs. [2] and [3]. Nevertheless, in the high Kubo number regime, the diffusion coefficient still increases with increasing gyroradii. The underlying physical mechanism for this effect could be identified as the broadening of the autocorrelation function due to the gyroaveraging of the potential. This is in contrast to Ref. [3] where the peculiar shape of the autocorrelation function has been made responsible for the increase. While the new method put forth in the present paper is compatible with the standard gyrokinetic way of working with gyroaveraged potentials, the previously published method is not.

4. Comparison of the DCT method with direct numerical simulations

4.1. General remarks

Given the fact that the DCT method is based on the *ad hoc* assumption expressed by Eq. (15), its validity can only be demonstrated *a posteriori* via comparisons with direct numerical simulations. However, no such attempt can be found in the literature. And the reason seems to be that the electrostatic potentials used for direct numerical simulations in the past either had autocorrelations that were too complicated for an efficient use of the DCT method or they did not satisfy the applicability conditions of the DCT method. The latter require that the statistics of the potential be homogeneous, stationary, and Gaussian. Such a potential can be generated by means of a superposition of a sufficiently large number of harmonic waves:

$$\phi(\mathbf{x},t)=\sum_{i=1}^{N}A_i\sin(\mathbf{k}_i\cdot\mathbf{x}+\omega_i t+\varphi_i)\,. \tag{25}$$

Its Gaussianity can be demonstrated with the help of the central limit theorem, regarding the characteristic numbers of the harmonic waves as a set of independent random variables. The autocorrelation function of such a potential is then easily shown to be

$$E(\mathbf{x},t)=\sum_{i=1}^{N}\frac{A_i^2}{2}\cos(\mathbf{k}_i\cdot\mathbf{x}+\omega_i t)\,. \tag{26}$$

Moreover, the effective correlations $E^{\mathrm{eff,A}}$ and $E^{\mathrm{eff,B}}$ are simply obtained by multiplying the individual Fourier components of E by $J_0(k_i\rho)$ and $J_0^2(k_i\rho)$, respectively.

As indicated above, an efficient use of the DCT method requires further that the autocorrelation be sufficiently smooth in space, i.e., it should not exhibit large spatial fluctuations. This is because the decorrelation trajectories $X(t;S)$ of neighboring subensembles should be similar in order to ensure convergence in the numerical solution of the integral in Eq. (16). As we have already mentioned, the advantage of the DCT method lies in replacing real chaotic trajectories by new deterministic decorrelation trajectories. However, for heavily oscillating autocorrelations, the latter become chaotic themselves. In this case, Eq. (16) cannot be solved any more since the number of subensembles is limited in practice. We are thus forced to employ a sufficiently large number of partial waves. We ended up using $N=10^5$ waves with a Gaussian amplitude spectrum of the form $A_i=A_{\max}\exp(-k_i^2/8)$. The wave numbers and frequencies are randomly and homogeneously distributed within the

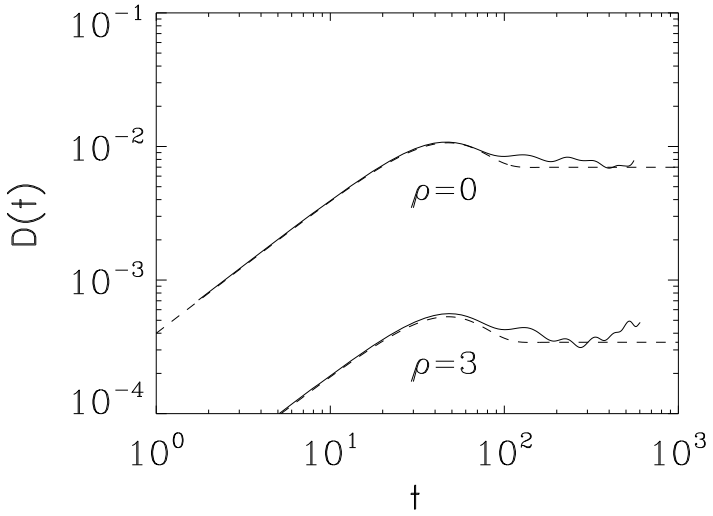

Figure 4. Time-dependent diffusivity $D(t)$ for $K = 0.18$: direct numerical simulation (———) and DCT method B (– – –).

intervals $0 \leq |\mathbf{k}_i| \leq k_{\max}$ and $0 \leq \omega_i \leq \omega_{\max}$. We note in passing that random distributions of wave numbers lead to much smoother autocorrelations than regular lattices in wave number space (see, e.g., Ref. [15]) and are therefore to be preferred. The Kubo number is controlled by varying $\omega_{\max}$. Due to this large number of partial waves, the autocorrelation function is fitted almost perfectly by a Gaussian of the form $E(\mathbf{x}) \propto \exp(-x^2)$. Isotropy leads to an important increase in efficiency by reducing the dimensionality of the subensemble space over which one has to integrate by one.

Given the large number of partial waves, it is not feasible any more to compute the potential or the autocorrelation anew for every time step of the numerical simulation. Instead, their values and those of the required derivatives are saved as three-dimensional arrays, e.g., $\phi(x_i, y_j, t_k)$. The values at intermediate space-time points are then recovered by means of cubic interpolations based on the well-known Lagrange formula. For solving the differential equations, a fourth-order Runge-Kutta method is used. The diffusivities are computed according to the definition given in Eq. (2). In order to obtain comparatively smooth curves, the ensemble average is calculated averaging a large number of different particle trajectories. Here, a number of some thousand trajectories has been found to be sufficient. A further improvement is obtained via the 'time average' method described in Ref. [15]. Here, the present positions of the particles are saved and reused as new starting points.

4.2. Numerical results

In Fig. 4, the time-dependent diffusion coefficient $D(t)$ is shown for $K = 0.18$ and $\rho = 0$ as well as $\rho = 3$. Length scales are again normalized with respect to the correlation length of the potential which is independent of the Kubo number. The DCT method B and the direct numerical numerical simulation agree fairly well in this low K regime. Moreover, in the finite gyroradius DCT case, both method B and method A lead to

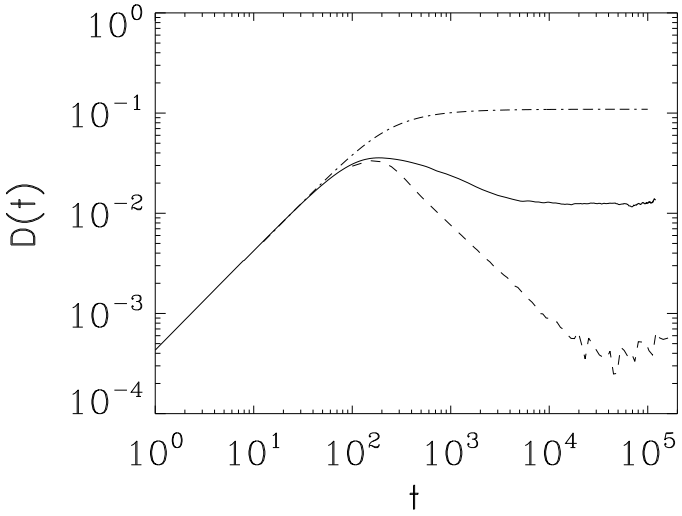

Figure 5. Time-dependent diffusivity $D(t)$ for $K = 180$ and $\rho = 0$: direct numerical simulation (———), DCT method B (− − −), and Corrsin approximation (− · − · −).

the same result (not shown). Of course, for $K < 1$, trapping effects are absent and the particles decorrelate temporary before they can explore the structure of the potential. Therefore the real question is how the DCT method performs at high Kubo numbers.

The behavior of the diffusivity for $K = 180$ and $\rho = 0$ is displayed in Fig. 5. Here, it is obvious that trapping effects influence the time evolution of the diffusion coefficient quite strongly. Interestingly, the curves obtained by direct numerical simulation and via the DCT method differ by more than one order of magnitude for large times. Indeed, the effect of trapping seems to be taken into account too strongly by the DCT method. As a further reference, the diffusion coefficient calculated with the Corrsin approximation [16] – a widely used approximation method which neglects trapping effects altogether – is also shown. The direct numerical simulation result is roughly half-way between those of the Corrsin approximation and the DCT method. The oscillations observed in the DCT curve for large times reflect once more the limited number of subensembles.

A comparison between direct numerical simulation and the DCT methods A and B for finite gyroradii ($\rho = 3$) is shown in Fig. 6. Method B again underestimates the transport level while method A greatly overpredicts it. While both DCT results deviate significantly from the exact one, this figure seems to suggest that the value obtained via the DCT method B is at least in the right ballpark while method A yields a number which is too large by about 1 1/2 orders of magnitude for this particular case. For large gyroradii and Kubo numbers, this difference increases further. Thus, the DCT approach A for particles with finite gyroradii must be discarded for two reasons: first, it is not in line with the physical principles underlying the $E\times B$ advection of particles with finite gyroradii, and second, it grossly overpredicts the transport levels in the high Kubo number regime. While surely not perfect, the DCT method B avoids this first drawback and also agrees much better with the direct numerical simulations.

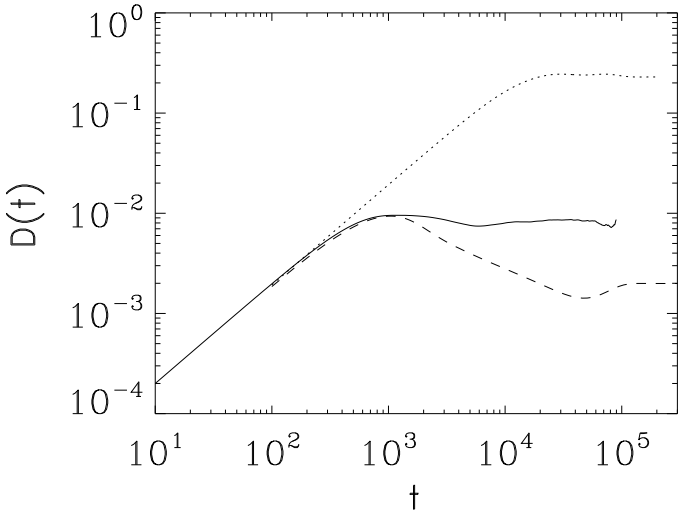

Figure 6. Time-dependent diffusivity $D(t)$ for $K = 180$ and $\rho = 3$: direct numerical simulation (———), DCT method B (– – –), and DCT method A (· · · · ·).

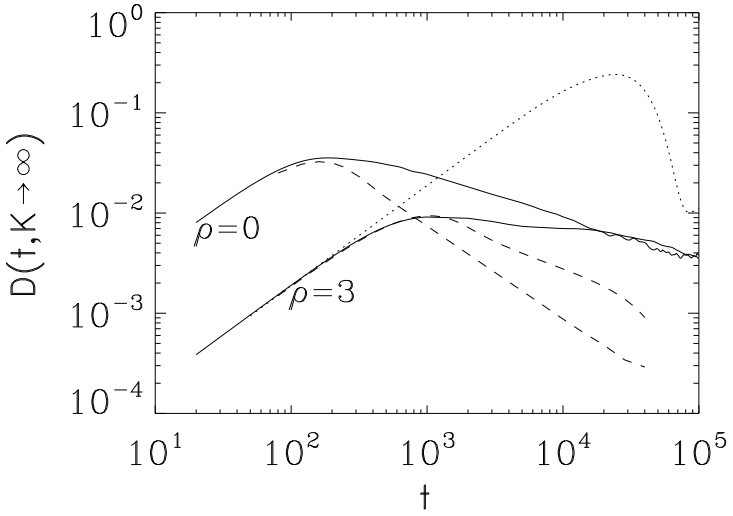

Figure 7. Time-dependent diffusivity $D(t)$ in a *static* potential, i.e., for $K \to \infty$: direct simulation (———), DCT method B (– – –), and DCT method A (· · · · ·).

This impression is confirmed in Fig. 7 which shows the time-dependent diffusivity for $\rho = 0$ and $\rho = 3$ in a *static* potential, i.e., for $K \to \infty$. The diffusion is subdiffusive in this case, with the direct numerical simulation and the DCT method B differing in their decay exponent in the large-time limit. [As mentioned before, this $D(t)$ curve

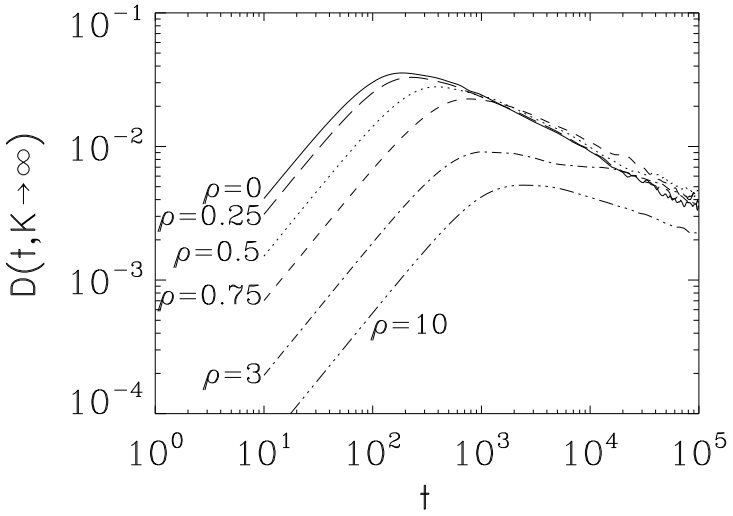

Figure 8. Time-dependent diffusivity $D(t)$ in a *static* potential, i.e., for $K \to \infty$, for different gyroradii ρ (normalized to the correlation length of the potential).

is related to $D(t \to \infty, K)$.] Again, the DCT method A yields anomalous results for $\rho > 0$.

We thus have to conclude that while the DCT method B works for small Kubo numbers, $K \lesssim 1$, it leads to quantitatively wrong results for $K \gtrsim 1$, i.e., in the nonlinear trapping regime. In contrast to the Corrsin approximation which is not able to describe the effect of particle trapping at all, the DCT method considers this effect too strongly. The reason for this behavior must lie in Eq. (15) which is the only major assumption in the DCT approach.

This finding leads us to consider direct numerical simulations of test particles with finite gyroradii in more detail in the following section. In this context we will find that despite its limits, the DCT method still provides both basic physical insight and some qualitative results which carry over to the exact treatment of this system. In particular, it will turn out that (1) a key effect at large Kubo numbers is the widening of the particle trajectories, and that (2) the narrowing of the gap between curves for different gyroradii in the high K regime [as observed in Fig. 7] persists.

5. Direct numerical simulations and analytical results for finite gyroradii

5.1. Results of direct numerical simulations

In the present section, we will concentrate on direct numerical simulations performed in a self-generated electrostatic potential described by Eq. (25). The time-dependent diffusion coefficient $D(t)$ for a static potential and for a set of different gyroradii is shown in Fig. 8. Here, the curves for $\rho = 0$ and $\rho = 3$ are the same as those in Fig. 7. Given the correspondence between $D(t, K \to \infty)$ and $D(t \to \infty, K)$ which has been mentioned several times already, one can expect the K-dependent long-time diffusivities to take on similar characteristics. This is indeed the case as can be inferred

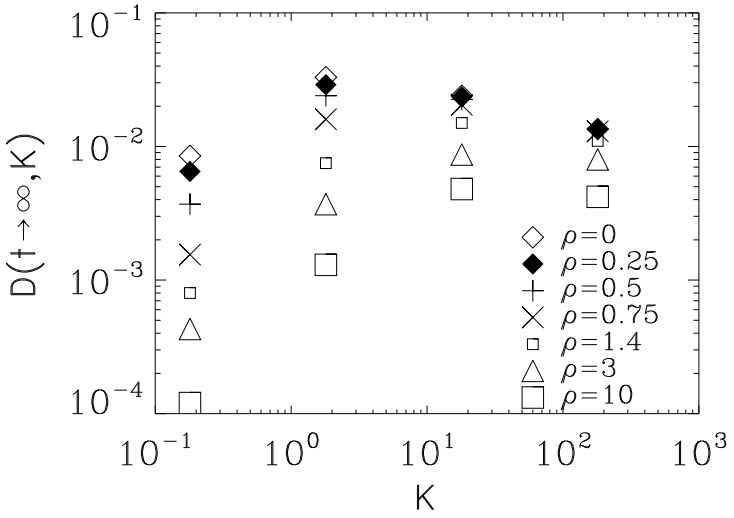

Figure 9. Long-time limit of the diffusivity D as a function of the Kubo number K for different gyroradii ρ (normalized to the correlation length of the potential).

from Fig. 9. Here, we plotted $D(t\to\infty, K)$ for several values of ρ (normalized, again, with respect to the correlation length of the potential). From Figs. 8 and 9, one can extract the scalings $D(t) \propto t$ and $D(K) \propto K$ for small times and small Kubo numbers, respectively, whereas for large times and large K, one finds $D(t) \propto t^{-0.4}$ and $D(K) \propto K^{-0.25}$. The latter scaling – which has a large error bar since it is based on only two points – is very close to Isichenko's estimate of $D(K) \propto K^{-0.3}$ which is based on percolation theory [17] (for numerical confirmations of this theory, see, e.g., Refs. [15, 18]). For small Kubo numbers, the transport is significantly reduced with increasing gyroradius even for $\rho \lesssim 1$. This behavior is in agreement with numerical simulations found in the literature (see, e.g., Ref. [10]). For larger Kubo numbers, $K \gtrsim 1$, the system's behavior is completely different, however. For $\rho \lesssim 1$, i.e., for gyroradii up to the correlation length, the transport is practically constant or even slightly increased with increasing ρ. In addition, the transport reduction with increasing ρ for $\rho \gtrsim 1$ is much slower than in the low Kubo number regime. These are key results of the present paper. They correct *both* the naive expectations *and* the previous DCT-based results. In the following, we shall develop an analytical approach which helps us to understand these findings both qualitatively and even quantitatively.

5.2. An analytical approach

As we have seen above, the DCT method tends to overemphasize trapping effects in the high Kubo number regime. Therefore the analytical description of the gyroradius dependence of the diffusivity which we are about to develop will be based directly on the effective autocorrelation function. From the latter, one can infer drift velocities and correlation lengths (as well as correlation times, of course) as a function of ρ. This information can in turn be used together with the well-known Kubo number scalings in the low and high K regimes to derive expressions for the gyroradius dependence of

the diffusivity. The formulas obtained this way will be shown to be in good agreement with the results from direct numerical simulations.

Qualitatively speaking, we will find the following scenarios in the case of small and large Kubo numbers. For $K \lesssim 1$, the situation is rather simple. The gyroaveraging merely smoothes out the potential and therefore reduces the effective drift velocity, leading to a significant reduction of the diffusion coefficient. For $K \gtrsim 1$, on the other hand, the presence of trapping effects introduces a new aspect. While the drift velocity is of course still reduced with increasing gyroradii, the gyroaveraging simultaneously enlarges the scales of the equipotential lines. Consequently, the gyrocenter trajectories become more extended, counteracting the reduction of the drift velocity. [A similar effect has been discussed before in the context of the DCT method.]

Starting from these ideas, the goal is to find analytical expressions for both the effective drift velocity V^{eff} and the average extension of a drift trajectory which will be assumed to scale like the correlation length λ_c^{eff}. An expression for the effective autocorrelation of the gyroaveraged potential has already been given in Eq. (23). For spatially isotropic autocorrelation functions as we are dealing with here, the angle between $\mathbf{x}$ and $\mathbf{k}$ can be integrated out, yielding

$$E_\rho^{\mathrm{eff}}(x) = \frac{1}{2\pi}\int_0^\infty dk\, k\, E(k)\, J_0^2(k\rho)\, J_0(kx)\,. \tag{27}$$

Assuming a Gaussian spatial autocorrelation of the form

$$E(x) = A\, e^{-x^2}\,, \tag{28}$$

which is in accordance with Eq. (26), we find

$$E_\rho^{\mathrm{eff}}(x) = \frac{A}{2}\int_0^\infty dk\, k\, e^{-k^2/4}\, J_0^2(k\rho)\, J_0(kx)\,. \tag{29}$$

Unfortunately, this integral cannot be solved analytically. However, the factor $J_0^2(k\rho)$ can be approximated in the limits of small and large arguments. E.g., for $k\rho \lesssim 1$, we find

$$J_0^2(k\rho) = 1 - (k\rho)^2/2 + 3\,(k\rho)^4/32 - 5\,(k\rho)^6/576 + \mathcal{O}(\rho^8) \tag{30}$$

by means of a Taylor expansion. In this case, Eq. (29) yields

$$\begin{aligned} E_{\mathrm{small}\,\rho}^{\mathrm{eff}}(x) = {} & A\, e^{-x^2} - 2A\rho^2\,(1-x^2)\, e^{-x^2} \\ & + \frac{3A\rho^4}{2}\,(2-4x^2+x^4)\, e^{-x^2} \\ & - \frac{5A\rho^6}{9}\,(6-18x^2+9x^4-x^6)\, e^{-x^2} + \mathcal{O}(\rho^8)\,. \end{aligned} \tag{31}$$

Using this expression, we then obtain

$$V_{\mathrm{small}\,\rho}^{\mathrm{eff}} = V\left[1 - 2\rho^2 + 5\rho^4/2 - 5\rho^6/3 + 5\rho^8/8 + \mathcal{O}(\rho^{10})\right] \tag{32}$$

for the effective drift velocity. Moreover, a perturbative calculation yields

$$\lambda_{\mathrm{small}\,\rho}^{\mathrm{eff}} = \lambda_c\left[1 + \rho^2 + \rho^4/4 + \mathcal{O}(\rho^6)\right] \tag{33}$$

for the effective correlation length. The factor $J_0^2(k\rho)$ in Eq. (27) suppresses shorter wavelengths and leads to an increase of the effective λ_c.

For $k\rho \gg 1$, on the other hand, the squared Bessel function is known to oscillate strongly. In this case, we thus approximate it by half of its envelope, i.e., we set

$$J_0^2(k\rho) \approx 1/(\pi k\rho)\,. \tag{34}$$

Eq. (29) then yields

$$E^{\mathrm{eff}}_{\mathrm{large}\,\rho}(x) = \frac{A}{2\sqrt{\pi}\rho}\, e^{-x^2/2}\, I_0\left(x^2/2\right)$$
$$= \frac{A}{2\sqrt{\pi}\rho}\, e^{-x^2/2}\, \left[1 + x^4/16 + x^8/1024 + \mathcal{O}(x^{12})\right] \tag{35}$$

where I_0 denotes the modified Bessel function of the first kind. From this expression, we obtain

$$V^{\mathrm{eff}}_{\mathrm{large}\,\rho} = V\,(4\sqrt{\pi}\rho)^{-1/2}\,. \tag{36}$$

Since the gyroradius ρ enters Eq. (35) just a prefactor, the effective correlation length is independent of it. The latter can be determined numerically to be

$$\lambda^{\mathrm{eff}}_{\mathrm{large}\,\rho} \approx 1.73\,. \tag{37}$$

For large gyroradii, the term $J_0^2(k\rho)$ in Eq. (27) reduces practically the entire k spectrum of the potential in the same way. Therefore the effective correlation length does not increase any more.

With the help of the above expressions for V^{eff} and λ_c^{eff} we are now able to estimate the resulting transport levels. In the limit of small Kubo numbers, $K \lesssim 1$, the diffusion coefficient is known to scale like $D \propto \lambda_c\, V\, K = \tau_c\, V^2$.[15, 18] Since the correlation time τ_c is not affected by the gyroaveraging, one only has to replace V by V^{eff} to obtain the corresponding diffusion coefficient for finite gyroradii. In the limit of large Kubo numbers, $K \gtrsim 1$, one has $D \propto \lambda_c\, V\, K^{\gamma-1} = \lambda^{2-\gamma} V^{\gamma} / \tau_c^{1-\gamma}$ instead.[15, 18] Due to trapping effects, one finds $\gamma < 1$. In Ref. [17], a consideration based on percolation theory suggests $\gamma = 0.7$, whereas we observe $\gamma \approx 0.75$ in our numerical simulations. It should be pointed out that in the large Kubo number regime, both the drift velocity *and* the correlation length are affected, namely in such a way that these two effects tend to cancel each other out. Employing the above formulas for V^{eff} and λ_c^{eff}, we finally obtain

$$D_\rho/D_0 \approx 1 + [2-3\gamma]\,\rho^2 + \left[\frac{3}{2} - \frac{21}{4}\gamma + \frac{9}{2}\gamma^2\right]\rho^4$$
$$+ \left[\frac{1}{2} - \frac{29}{12}\gamma + \frac{27}{4}\gamma^2 - \frac{9}{2}\gamma^3\right]\rho^6 \quad \text{for } \rho \lesssim 1 \tag{38}$$

and

$$D_\rho/D_0 \approx 1.73^{2-\gamma}\,(4\sqrt{\pi}\rho)^{-\gamma/2} \quad \text{for } \rho \gg 1 \tag{39}$$

where $\gamma = 2$ for $K \lesssim 1$ and $\gamma \approx 0.75$ for $K \gtrsim 1$. It is interesting to note that for $\gamma = 2/3$, the second and fourth order terms in Eq. (38) vanish exactly, i.e., D_ρ/D_0 is constant for small values of ρ up to sixth order corrections. Since this critical value for γ is pretty close to both ours ($\gamma \approx 0.75$) and Isichenko's ($\gamma = 0.7$) in the large Kubo number regime, the diffusivity depends only weakly on the gyroradius in this case as long as it is smaller than or comparable to the correlation length. This confirms our simulation results in the $K \gg 1$ limit. In the low K regime, we find $D_\rho/D_0 \approx 1 - 4\,\rho^2$ instead, and for large gyroradii, the transport is reduced with increasing ρ like ρ^{-1} or $\rho^{-\gamma/2}$ for $K \lesssim 1$ or $K \gtrsim 1$, respectively. The simulation results shown in Fig. 9 are compared to the analytical approximations in Fig. 10. In general, we find fairly good agreement for both small and large gyroradii. Only for $K = 180$ and $\rho = 10$, the numerical value is somewhat smaller than the analytical one. In this case, the nonlinear regime is not fully established yet due to the strongly reduced drift velocity.

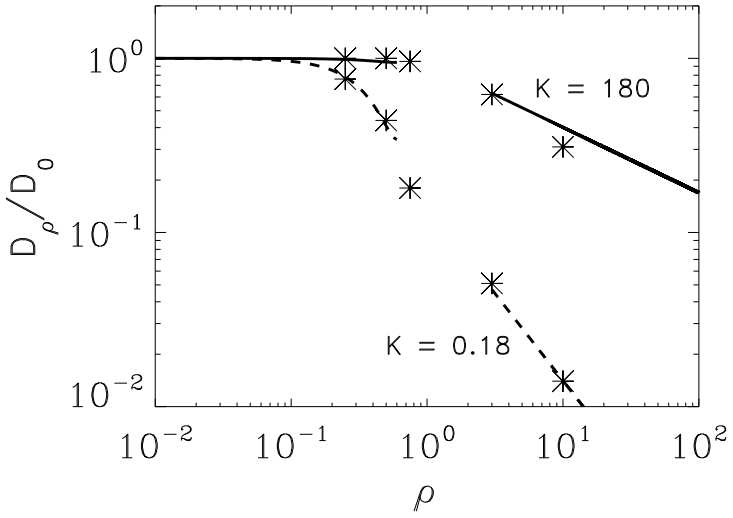

Figure 10. Comparison between the numerically determined diffusion coefficients and the analytical formulas, Eqs. (38) and (39). Here, D_0 and D_ρ denote, respectively, the diffusivity for vanishing and finite gyroradius.

6. Conclusions

In summary, we have used a modified decorrelation trajectory (DCT) approach, direct numerical simulations, and analytical analysis to establish a rather detailed and coherent picture of the turbulent advection of test particles with finite gyroradii. Our results correct *both* the naive expectations *and* the previously published DCT-based results.[2, 3] While in the low Kubo number (weak turbulence) regime, the diffusivity falls off rapidly with increasing gyroradius, it is more or less constant in the high Kubo number (strong turbulence) regime as long as the gyroradius does not exceed the correlation length of the electrostatic potential. The physical mechanisms underlying these results were identified and discussed. In particular, we found that for $K \gtrsim 1$, the decrease of the average drift velocity with increasing gyroradius tends to be balanced by an increase of the effective correlation length. Thus the particles are able to travel larger distances, and the diffusivity is practically left unchanged. If the gyroradius clearly exceeds the correlation length, on the other hand, the diffusivity falls off as $\rho^{-\gamma/2}$ with $\gamma = 2$ for $K \lesssim 1$ and $\gamma \approx 0.75$ for $K \gtrsim 1$. This is consistent with previous studies of test particle diffusion in Hasegawa-Mima turbulence.[11]

While the main purpose of the present paper was to investigate the fundamental physical processes responsible for the gyroradius dependence of the diffusivity under various circumstances, it is easy to envision possible applications both in fusion research and in plasma astrophysics. Although additional effects might enter in these cases, the basic mechanisms discussed in this paper are expected to remain relevant. E.g., to assess the interaction of fusion α particles with the background microturbulence in future burning plasma experiments, one requires the insights and results presented in Sections 3-5. Based on simulations with the nonlinear gyrokinetic code `gene` [19, 20], we expect the Kubo numbers under realistic experimental

conditions to be of the order of unity or even slightly larger. At the same time, the gyroradii of the energetic α particles will probably not exceed the correlation length of the electrostatic potential. Consequently, it is reasonable to expect that the finite Larmor radius reduction of the turbulent diffusion is rendered ineffective, suggesting a significant impact of the turbulence on the α particle transport.

[1] E. A. Frieman and L. Chen, Phys. Fluids **25**, 502 (1982).
[2] M. Vlad and F. Spineanu, Plasma Phys. Control. Fusion **47**, 281 (2005).
[3] M. Vlad, F. Spineanu, S. I. Itoh, M. Yagi, and K. Itoh, Plasma Phys. Control. Fusion **47**, 1015 (2005).
[4] M. Vlad, F. Spineanu, J. H. Misguich, and R. Balescu, Phy. Rev. E **58**, 7359 (1998).
[5] M. Vlad, F. Spineanu, J. H. Misguich, J. D. Reuss, R. Balescu, K. Itoh, and S. I. Itoh, Plasma Phys. Control. Fusion **46**, 1051 (2004).
[6] M. Vlad and F. Spineanu, Phys. Rev. E **70**, 056304 (2004)
[7] R. Balescu, *Aspects of Anomalous Transport in Plasmas* (IoP Publishing, Bristol, 2005).
[8] V. Naulin, A. H. Nielsen, and J. J. Rasmussen, Phys. Plasmas **6**, 4575 (1999).
[9] B. Scott, Phys. Plasmas **12**, 082305 (2005).
[10] G. Manfredi and R. O. Dendy, Phys. Rev. Lett. **76**, 4360 (1996).
[11] G. Manfredi and R. O. Dendy, Phys. Plasmas **4**, 628 (1997).
[12] S. V. Annibaldi, G. Manfredi, and R. O. Dendy, Phys. Plasmas **9**, 791 (2002).
[13] G. I. Taylor, Proc. Lond. Math. Soc. **20**, 196 (1920).
[14] R. Kubo, J. Math. Phys. **4**, 174 (1963).
[15] J. H. Reuss, J. D. and Misguich, Phys. Rev. E **54**, 1857 (1996).
[16] S. Corrsin, in: F. Frenkiel and P. Sheppard, *Atmospheric Diffusion and Air Pollution* (Academic Press, New York, 1959).
[17] M. B. Isichenko, Rev. Mod. Phys. **64**, 961 (1992).
[18] J. D. Reuss, M. Vlad, and J. H. Misguich, Phys. Lett. A **241**, 94 (1998).
[19] F. Jenko, W. Dorland, M. Kotschenreuther, and B. N. Rogers, Phys. Plasmas **7**, 1904 (2000).
[20] T. Dannert and F. Jenko, Phys. Plasmas **12**, 072309 (2005).